ISIJ International, Vol. 52 (2012), No. 12, pp. 2278–2282

A Simple Model for Abnormal Grain Growth

Mohammad Abdur RAZZAK,[1)]* Michel PEREZ,[1)] Thomas SOURMAIL,[2)] Sophie CAZOTTES[1)] and Marion FROTEY[2)]

1) Université de Lyon - INSA Lyon - MATEIS - UMR, CNRS 5510 - F69621 Villeurbanne - France.
2) Ascometal CREAS, BP 70045, 57301 Hagondange, Cedex, France.

(*Received on April 19, 2012; accepted on July 25, 2012*)

A new approach to predict the propagation of abnormal grain growth is presented. The growth rate of an existing large (abnormal) grain is compared to the growth rate of the surrounding (normal) grains. A very simple argument based on the reduction of grain boundary surface serves as driving force, whereas the pinning force is due to second phase precipitates. The model is successfully tested and validated on a low alloy steel presenting various state of precipitation depending on thermal history.

KEY WORDS: abnormal grain growth; modeling; pinning; low alloy steels.

1. Introduction

Grain size control is an important issue in materials science. The direct impact of grain size on mechanical properties of materials derived fundamental and applied research on grain growth phenomenon. Normal grain growth in materials is defined when the grain size distribution remains quasi-stationary during the coarsening phenomenon.[1)] Abnormal Grain Growth (AGG) is defined as the growth of few number of grains more rapidly in comparison with the others. A microstructure subjected to AGG has the characteristics of having very large grains surrounded by relatively much smaller grains.[2)]

There are numbers of authors who have been able to deduce the parabolic grain growth relationship for mean grain size in the case of normal grain growth (see the pioneer paper of Hillert[3)] and the review of Gladman[2)]). Subsequently these models were extended to predict and explain AGG in materials. M. Hillert addressed the "abnormal" or "discontinuous" grain growth phenomenon as a defect model.[3)] In his model the growing and shrinking grains are determined by the number of neighbors it has.

The causes of AGG are not yet very well understood. Some authors claim that AGG is due to variable grain boundary mobility (*e.g.* induced by texture).[4)] Whereas others cite second phase particles (*i.e.* precipitates) as the cause of AGG.[1,5)]

Andersen *et al.*[1)] proposed a 2D analytical model in which, an abnormal grain is surrounded by an array of hexagonal grains. Andersen proposed a grain growth mechanism map, in which AGG occurs when (i) smaller grains are pinned, and, (ii) the abnormal grain is large enough compared to the normal grains.

Bréchet and Militzer[5)] proposed a deviation from the normal Zener pinning formalism. They suggested that the particles located at corner points or quadruple points have higher pinning effciency than particles evenly distributed in the matrix. As the number of corner points depends on the grain size, the pinning force also becomes dependent on the grain size, leading to an instability domain, for which the larger the grains are, the faster they grow. More recent experimental work done by Leguen[6)] showed that precipitate size distribution is a key parameter in AGG onset.

In this paper, we propose a criterion for AGG propagation in the presence of second phase precipitates. Based on 3D geometrical considerations, a simple model to predict the stability of an existing AGG situation will be presented. Grain boundary pinning is assumed to occur by both classical Zener mechanism and corner point pinning. This model aims at predicting the conditions, in term of precipitation state, for which AGG may occur and propagate.

2. Mathematical Derivation

Grain growth theory is basically based on the decrease in grain boundary interfacial energy being the driving force. In the case of AGG the driving pressure of the abnormal grain is larger than the one of neighboring grains and finally consumes them. In the present case the grains are represented as sphere (see **Fig. 1**). A large grain of diameter D_{ab} (the abnormal grain) is surrounded by smaller (normal) grains of diameter D_n (state ①). In a thermally activated evolution the abnormal grain can increase its diameter at the detriment of surrounding normal grains and attain a new diameter of $(D_{ab} + 2D_n)$ (state ②). The total work $\delta W = E_1 - E_2$ done to move the system from initial energy state ① E_1 to state ② E_2 determines the driving pressure P_{ab} for the abnormal grain to grow (as shown in Fig. 1), such as $\delta W = P_{ab} dV$. Here dV is the volume change of the abnormal grain from state ① to state ②. it is given by: $\delta V = \lambda_{ab} D_{ab}^2 \delta D_{ab} / 2$, where λ_{ab} is a geometric factor ($\lambda_{ab} = \pi$ for a sphere).

The total number of normal grains n_n surrounding the

* Corresponding author: E-mail: mohammad.razzak@insa-lyon.fr
DOI: http://dx.doi.org/10.2355/isijinternational.52.2278

abnormal grain depends on D_n and D_{ab}. It can be estimated as the ratio of the total available surface around the abnormal grain over the projected surface of a normal grain:

$$n_n = \rho \frac{\lambda_{ab}(D_{ab}+D_n)^2}{\lambda_p \lambda_n D_n^2} = 4\mu \frac{\lambda_{ab}}{\lambda_n} \frac{(D_n+D_{ab})^2}{D_n^2} \quad \text{... (2.1)}$$

where ρ is the compact effciency factor, λ_n is a geometric factor ($\lambda_n = \pi$ for a sphere), λ_p is the ratio of the projected surface over the actual surface of normal grains ($\lambda_p = 1/4$ for a sphere) and $\mu = \rho/(4\lambda_p)$ which has a value ranging from 0.5 to 0.8. The total interfacial energy of state ① (see Fig. 1) is then:

$$E_1 = \frac{\gamma}{2}\left[\lambda_{ab} D_{ab}^2 + n_n \lambda_n D_n^2\right] = \frac{\gamma \lambda_{ab}}{2}\left[D_{ab}^2 + 4\mu (D_{ab}+D_n)^2\right] \quad \text{..... (2.2)}$$

where γ is the grain boundary interfacial energy. Similarly, the total interfacial energy of the state ② (see Fig. 1) is:

$$E_2 = \frac{\gamma \lambda_{ab}}{2}\left[D_{ab} + 2D_n\right]^2 \quad \text{..... (2.3)}$$

Driving pressure of abnormal grain growth is determined by:

$$P_{D_{ab}} = \frac{\delta W}{\delta V} = \frac{E_1 - E_2}{\delta D_{ab}} \frac{\delta D_{ab}}{\delta V} = \frac{E_1 - E_2}{2D_n} \frac{2}{\lambda_{ab} D_{ab}^2} \quad \text{... (2.4)}$$

giving thus for the abnormal grain driving pressure:

$$P_{D_{ab}} = \frac{2\gamma}{D_n}\left[\mu - (1-\mu)\left(\frac{D_n}{D_{ab}}\right)^2 + (2\mu - 1)\frac{D_n}{D_{ab}}\right] \quad \text{... (2.5)}$$

The grain coarsening phenomenon implies that the grain boundaries move through the matrix. In the presence of second phase particles there is always a possibility that the grain boundary will eventually meet the second phase particles.

Zener showed that second phase particles produce back stress which can hinder the boundary movement. A a particle of radius r exerts a force $f_z = k_s r \gamma$ on the grain boundary, where k_s is a geometrical factor, having a value of π for spherical particles. Assuming a random distribution, the number density of second phase particles (N) is related to the precipitate volume fraction (f) by $f_z = N k_v r^3$, where k_v is another geometrical factor, having a value of $4\pi/3$ for spherical particles. Finally, the number n_s of particles interacting with 1 m^2 of grain boundary is $n_s = 2rN$ and the pinning pressure is:

$$P_Z = n_s f_z = \frac{2k_s \gamma f}{k_v r} \quad \text{..... (2.6)}$$

Now, if we consider the distribution of the second phase particles, the precipitate size distribution is described by n classes of radii r_i populated with n_i precipitates per unit volume. From the knowledge of the precipitate size distribution (*i.e.* the function $n_i(r_i)$), the total pinning pressure is simply the sum over the pinning pressure of each precipitate size class:

$$P_Z = \sum_i^n 2r_i n_i k_s r_i \gamma = 2k_s \gamma N_r \text{ where, } N_r = \sum_i^n n_i r_i^2 \quad \text{..... (2.7)}$$

Note that the classical Zener pinning pressure does not depend on the grain size distribution. However, the driving pressure for normal grain growth does depend of grain size. It is usually given by $P_{Dn} = \lambda\gamma/D_n$, where λ is a constant. Zener and Gladmann[2] proposed originally of value of 4 for λ in comparison with the pinning force. More recently, based on many experimental results, Rios[7] proved a more accurate expression to be 8 times smaller than ZenerâĂŹs. In the following, we take $\lambda = 0.5$. The grains are therefore supposed to grow until they reach a limiting size of D_n^l, for witch the driving pressure equals the pinning pressure, leading to:

$$P_Z = \frac{\lambda\gamma}{D_n^l} \text{ with } D_n^l = \frac{\lambda k_v}{2k_s N_r} \quad \text{..... (2.8)}$$

The limiting grain size D_n^l is often used as a parameter to quantify the pinning effciency of a second phase particle distribution.

Considering Zener pinning pressure over all the grains, a simple expression for the grain growth rate can be written as:

$$\frac{dD_{ab}}{dt} = M\left(P_{D_{ab}} - P_Z\right) \quad \text{..... (2.9)}$$

Here, $M = M_0 \exp\left(-\frac{Q}{RT}\right)$. M is the mobility of the grain boundary, Q is the activation energy, R is the molar gas constant, T is temperature and M_0 is a pre-exponential factor. The same expression holds for normal grain growth:

$$\frac{dD_n}{dt} = M\left(P_{D_n} - P_Z\right) \quad \text{..... (2.10)}$$

The two conditions for AGG are then classically stated as follows:

$$\frac{dD_{ab}}{dt} > 0 \text{ and } \frac{d}{dt}\left(\frac{D_{ab}}{D_n}\right) > 0 \quad \text{.....(2.11)}$$

From Eqs. (2.5), (2.8), (2.9) and (2.10), and posing $x = D_n / D_n^l$ and $y = D_{ab}/D_n$, the two conditions for AGG can be written as:

$$\mu - (1-\mu)y^{-2} + (2\mu - 1)y^{-1} - x\lambda/2 > 0 \quad \text{..... (2.12)}$$

$$\mu - (1-\mu)y^{-2} + (2\mu - 1)y^{-1} - \lambda/2\left[x + y(1-x)\right] > 0 \quad \text{..... (2.13)}$$

Equations (2.12) and (2.13) can be solved numerically. Results obtained over a range of x and y yield tentative conditions for normal and AGG.

3. Mechanism Map with Zener Pinning

Solutions of Eqs. (2.12) and (2.13) are plotted in **Fig. 2** showing the mechanism map of AGG for $\mu = 0.5$ as a function of $x = D_n / D_n^l$ (pinning pressure) and $y = D_{ab}/D_n$ (initial size of the instability). As expected, the growth of the abnormal grain (dD_{ab}/dt) is hindered by second phase particles pinning and favored when the contrast between normal and abnormal grains is large (higher driving force). However, as the abnormal grain becomes larger, the *relative* driving force for normal grains to grow also increases. The *relative* growth of the abnormal grains ($d(D_{ab}/D_n)/dt$) is then favored

when (i) the pinning pressure is high and (ii) the size of the abnormal grain relative to normal grains is moderate. Ideal conditions for AGG seem to be the same as ideal conditions to have small grains. In other words, the price to pay to keep

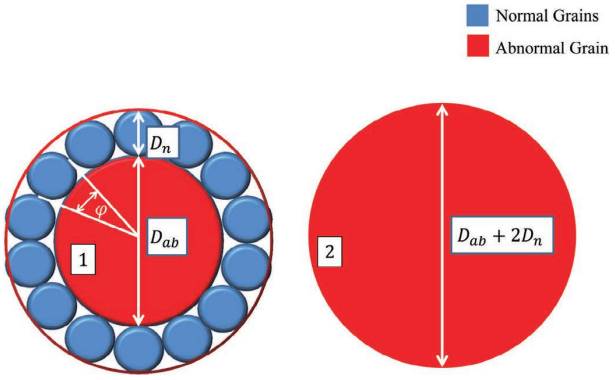

Fig. 1. Schematic representation of an abnormal grain of diameter D_{ab} surrounded by normal grain, of diameter D_n. The abnormal grain is growing from state (1) to state (2) by consuming all the surrounding normal grains and increasing its diameter by $2D_n$.

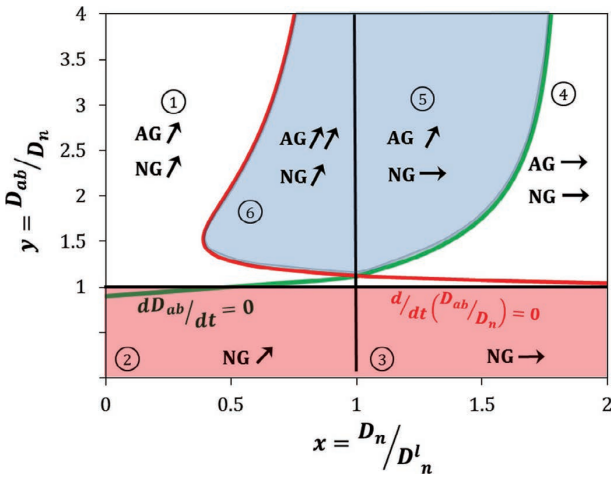

Fig. 2. Mechanism map for AGG considering Zener pinning with $\mu = 0.5$ and $\lambda = 0.5$. The map exhibits 6 domains ①: normal and abnormal grains grow in a stable manner, ②: normal grains can grow, ③: normal grains are pinned, ④: both abnormal and normal grains are pinned, ⑤: normal grains are pinned, whereas the abnormal grain grows (unstable AGG region) and ⑥: normal and abnormal grains grow in an unstable manner (unstable AGG region). y scale is valid above the red shaded area from $y = 1$.

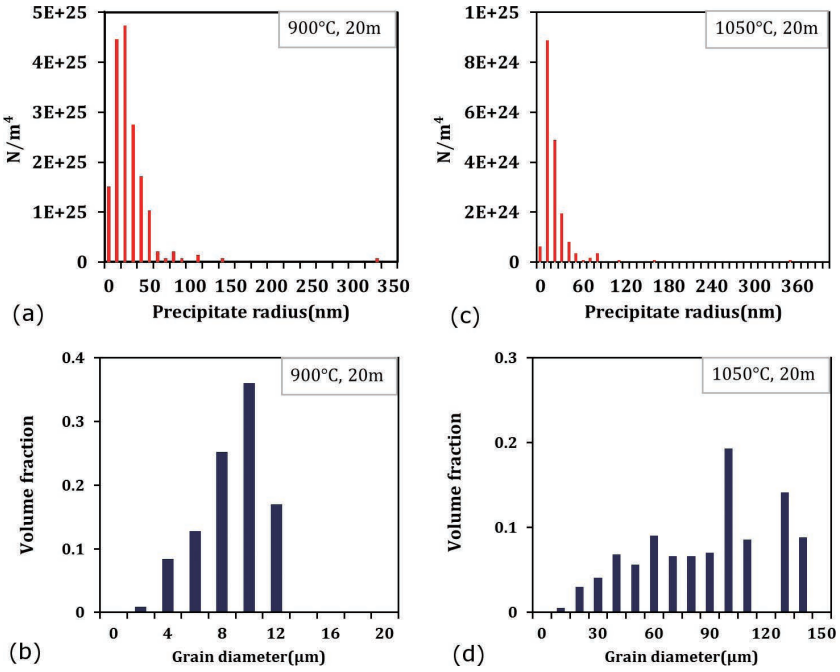

Fig. 3. (a) Precipitates size distribution of FeVNbCN alloy heat treated at 900°C for 20 minute, (b) Grain size distribution corresponding the state (a), (c) Heat treated at 1 050°C for 20 minute, (d) Grain size distribution corresponding to (c).

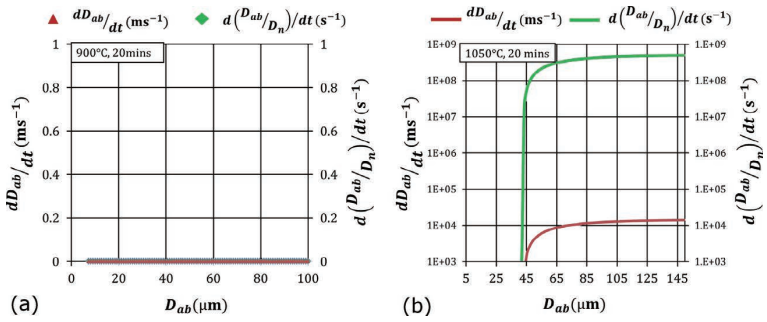

Fig. 4. (a) FeVNbCN alloy heat treated at 900°C for 20 minute (No AGG). (b) Heat treated at 1 050°C for 20 minute (Presence of abnormal grains). Here, the grain boundary mobility is $M = 1$ m^2/s, $\mu = 0.5$ and $\lambda = 0.5$.

a fine microstructure is a potentially leads to unstable situation.

It is remarkable how similar the present mechanism map looks like, compared to Andersen's *et al*.[1] In the limiting case where D_n / D_n^l approaches unity, we found that an abnormal grain with a size advantage greater than about $1.4D_n$ ($\mu = 0.5$) to $2D_n$ ($\mu = 0.6$) will continue to grow abnormally. Anderson *et al.* found a value of $1.4D_n$.

4. Zener and Corner Pinning by Second Phase Particles

Bréchet *et al.*[5] proposed that particles lying on the triple junctions or quadruple points (special location) are more effective in pinning the boundary movement than particles lying on the boundary. Their pinning force being $f_c = \alpha_0 f_z$, where α_0 is a constant larger than 1. They considered that quadruple points are preferential location for precipitates: *i.e.* if the number of precipitates is large enough, all corner points will be occupied, whereas remaining particles participate in classical Zener pinning. From the grain size, they estimated the number of quadruple points and proposed an expression for the net pinning force being the addition of corner point pinning and Zener pinning.

It has been shown elsewhere[6] that, in some cases, the precipitate population is poorly described by taking only averaged quantities, *i.e.* mean radius instead of the whole distribution. In this paper, corner point pinning will be considered taking into account the whole precipitate size distribution.

From Eq. (2.7) it is apparent that larger precipitates create higher pinning force. So, it can be assumed that grain boundaries hinder on the larger particles subsequently become the triple junction or corner point. The assumption that special location is created at the larger particles creates a guideline for further evolution of modeling concept using particles size distribution. In this model, it is assumed that the larger particles occupy the special location preferentially. After filling all the special location in descending diameter, the rest of the precipitates participate in conventional Zener pinning in the matrix.

In a matrix where an abnormal grain of diameter, D_{ab} is surrounded by normal grains of diameter D_n, the number of corner points per unit volume $N^* = K_0 / (K_V D_n^3)$, where K_0 is the number of corner point per grain and K_V is a geometrical factor.

Let consider a particles size distribution $n_i(r_i)$ with a total number of precipitates $n_n = \sum_i n_i$. As stated before larger particles reside in the special locations, whereas smaller ones go to the conventional Zener pinning. There should be a critical radius r_c of the particles where the partitioning between particles occurs for Zener and corner point pinning. As reported by Bréchet *et al*. the pinning force is dependent on the number of the corner points available in the system. If $n_n < N^*$:

$$P_C = \sum_i \frac{n_i}{N^*} \frac{K_0 \alpha k_s \gamma r_i}{K_A D_n^2} = \frac{K_V \alpha k_s \gamma}{K_A} D_n \sum_{i=1}^{n} n_i r_i \quad \text{..... (4.1)}$$

If $n_n > N^*$, the total pinning force is given by P_C and P_Z:

$$P_C = \frac{K_V \alpha k_s \gamma}{K_A} D_n \sum_{i=i^*}^{n} n_i r_i \text{ and } P_Z = 2k_s \gamma \sum_{i=1}^{i^*} n_i r_i^2 \quad \text{..... (4.2)}$$

where i^* is the index of the precipitate class from which precipitates are either lying in corner points or involved in classical Zener pinning. As the pinning force of precipitate in corner points is $f_C = \alpha_0 k_s \gamma r_i$, larger precipitates have a higher probability of lying at corner points. Therefore, smaller precipitates of class index 1 to i^* are involved in classical Zener pinning whereas larger precipitates of class index i^* to n are lying in corner points:

$$\sum_{i=i^*}^{n} n_i < N^* < \sum_{i=i^*-1}^{n} n_i \quad \text{..... (4.3)}$$

Note that i^* depends on D_n: the smaller is D_n, the larger is N^* and, consequently, the smaller is index i^*. Considering corner and Zener pinning simultaneously Eqs. (2.9) and (2.10) are modified as follows:

$$\frac{dD_{ab}}{dt} = M\left[P_{D_{ab}} - P_C - P_Z\right] \quad \text{..... (4.4)}$$

$$\frac{dD_n}{dt} = M\left[P_{D_n} - P_C - P_Z\right] \quad \text{..... (4.5)}$$

The second condition, $\frac{d}{dt}\left(\frac{D_{ab}}{D_n}\right)$ for abnormal grain growth can be expressed in terms of Eqs. (4.4) and (4.5) as follows:

$$\frac{d}{dt}\left(\frac{D_{ab}}{D_n}\right) = \frac{1}{D_n}\frac{dD_{ab}}{dt} - \frac{D_{ab}}{D_n^2}\frac{dD_n}{dt} \quad \text{..... (4.6)}$$

Including corner pinning force increases the total pinning force in the system. Abnormal grain's critical diameter is determined by the equilibrium between the growth pressure and pinning pressure. Increase in pinning pressure eventually leads to smaller critical diameter than the first case, where only Zener pinning is considered.

5. Application to a Low Alloyed Steel

To validate the proposed approach, a model Fe–0.0071 at%Nb–0.217 at%V–2.2 at%C–0.025 at%N alloy was studied. This alloys was submitted to an austenitizating treatment (10 Day at 800°C) and then quenched in water. A subsequent heat treatment at various temperatures ranging from 900 to 1 200°C was performed in order to study the effects of the dissolving precipitate population on austenite grains size distribution.

In **Fig. 3**, precipitate and grain size distribution are presented for two heat treatments: 20 min at 900°C (Figs. 3(a) and 3(b)) and 20 min at 1 050°C (Figs. 3(c) and 3(d)). From metallographic observation (with an adequate Béchet-Baujard etching revealing prior austenite grains) it was seen, that samples heat treated 20 min at 900°C showed no AGG, while the 1 050°C for 20 min heat treated condition showed pronounced AGG in the microstructure. The AGG phenomenon is also clearly visible on the grain size distribution (Fig. 3(d)) as the volume fraction of the larger grains are much higher than the average grain size (28 μm).

The presented model is applied to predict the AGG phenomenon in the FeNbVCN model alloy where the precipitates size distribution and mean grain size is taken as the input parameters. Precipitates distribution along with mean

Table 1. List of zener and corner pinning values with the grain growth criteria of the corresponding heat treated state.

Heat treated state	D_n (μm)	P_C (Nm^{-2})	P_Z (Nm^{-2})	D_n^l (μm)	Growth criteria
900°C-2 min	6	5.95E05	8.87E4	1.0	NGG
900°C-20 min	6	5.61E11	3.22E11	~0.0	NGG
900°C-200 min	6	1.42E5	3.72E4	3.0	NGG
1 050°C-2 min	14	1.58E4	1.45E3	29	AGG
1 050°C-20 min	28	1.94E4	9.81E2	25	AGG
1 050°C-200 min	38	1.16E4	7.00E2	41	AGG

Table 2. List of all the model parameters used in the calculation.

k_s[5)]	k_v[5)]	λ_n	γ	α	K_V[5)]	K_A[5)]
π	$4\pi/3$	0.6	1	2	$(1.1)^3\pi/6$	$(1.1)^2\pi/2$

grain size of the samples heat treated at 900°C and 1 050°C for 2, 20 and 200 min are taken as input parameters to verify the model and estimate its affectivity in predicting the occurrence of AGG. In all the studied case, zener pinning along with corner pinning is taken into account to estimate the total pinning pressure in the system. The step by step procedure can be described as follows where the model parameters used in listed in **Table 2**;

1. The number of corner points in the system is calculated using, $N^* = K_0 / (K_V D_n^3)$ relation where D_n is the mean grain diameter.
2. Starting from the class of precipitates with largest radius (furthest right of the distribution) as shown in **Fig. 4**, the number of corner point available is filled with the corresponding and also subsequent classes of precipitates. The corner point pinning pressure for individual class is calculated using the Eq. (4.1).
3. After utilizing the largest radius classes of precipitates in the corner point pinning, the rest of the classes of precipitates are taken into account for zener pinning. The zener pinning pressure for individual class is calculated using the Eq. (4.2).
4. Growth pressure for individual D_{ab}^i starting from $D_{ab}^1 = D_n$ to $D_{ab}^{end} = 100 \times D_n$ is calculated following the Eq. (4.4). In parallel growth pressure of the normal grains are calculated using the Eq. (4.5). Growth rate of the larger grains $\frac{dD_{ab}}{dt}$ and normal grains $\frac{dD_n}{dt}$ is used in the Eq. (4.6) to measure the instability of the system to predict abnormal grain growth in the system.

In the **Table 1** pinning force along with grain growth criterion of the six states are listed. Among the results, two of them are presented in detail 900°C (20 min) and 1 050°C (20 min) (see Fig. 4).

Figure 4 represents abnormal (Eq. (4.4)) and relative (Eq. (4.6)) grain growth rates as a function of initial abnormal grain size. Following the conditions presented in expression (2.11), it can be seen in Fig. 4 that no AGG should be observed for the 900°C (20 min) treatment, whereas AGG should occur for grains larger than ~28 μm for the 1 050°C (20 min) treatment. It is notable that grains larger than ~28 μm exist (see the distribution on Fig. 3(d)) and that AGG is also observed from metallographic analysis.

This analysis has been performed for six heat treatment conditions without changing model parameters (μ = 0.5 and λ = 0.5). In order to represent the abnormal grain growth criterion, it is not required to utilize the experimentally determined mobility. So, grain boundary mobility M = 1 m^2/s is used in the calculation. For all of them, the model predictions were in agreement with the metallographic observation.

6. Conclusion

In the present model, AGG is handled with simple geometrical assumptions: one abnormal grain surrounded by normal grains. If only Zener pinning occurs, a mechanism map for normal and abnormal grain growth has been presented. It shows that AGG occurs for highly pinned conditions. The derived model was improved in order to take into account corner pinning (pinning at quadruple point junctions) and finally applied to a low alloy steel for various heat treatments and various precipitate size distributions.

With only one set of model parameters, the model is able to predict AGG for all studied heat treatments, with the possibility to indicate from which grain size is susceptible to AGG.

REFERENCES

1) I. Andersen, O. Grong and N. Ryum: *Acta Metall. Mater.*, **43** (1995), 2689.
2) T. Gladman: The Physical Metallurgy of Microalloyed Steels, The Instute of Materials, London, (2002).
3) M. Hillert: *Acta Metall.*, **13** (1965), 227.
4) A. D. Rollett and W. Mullins: *Scr. Mater.*, **36** (1997), 975.
5) Y. Bréchet and M. Militzer: *Scr. Mater.*, **52** (2005), 1299.
6) C. Leguen, M. Perez, T. Epicier, D. Acevedo and T. Sourmail: *Acta Mater.*, (2010), submitted.
7) P. Rios: *Acta Metall.*, **35** (1987), 2805.